16th ICAAR LISBOA 2020-2022

16th International Conference on
Alkali-Aggregate Reaction in Concrete
Lisboa | LNEC | Portugal | 31 May - 2 June 2022

Technical Visit

3 to 5 June 2022

1. Brief geology of Portugal

Mainland Portugal has a remarkable geological heterogeneity with formations ranging from the Precambrian to the Quaternary. The territory is divided into three major structural units, which, in turn, are subdivided into several zones, according to geological and structural characteristics. These features also molded the geomorphology of the land, as can be observed in Fig. 1.

The Hesperic Massif is a wide area composed by igneous and metasedimentary rocks from Precambrian and Palaeozoic age. This area comprises most Mainland Portugal and the eastern part of Spain. The Portuguese part of the massif is also divided into several units with different geological characteristics and ages. The Portuguese northern part of the massif is mostly composed by granitoid rocks and schists. The NNE-SSW fracture system Régua-Verin-Penacova and the Vilariça fault (Ribeiro et al., 1979) are the main structural features of the region. These fault systems are known to play an important role in the regional deep circulation of mineral waters, with the occurrence of springs along them.

The southern part of the Portuguese segment of the Iberian Massif is formed by two geotectonic units, comprising Precambrian and Lower Palaeozoic rocks showing intense deformation caused by different deformation phases with distinct trends and widespread volcanic synorogenic magmatism. In the NE part of the area granitoid rocks occur.

In the areas of predominance of granitic and schistose rocks, and in the central zone, the Schist-Greywacke Complex (SGC) occupies a large area. Ordovician rocks, comprising thick layers of massive quartzite, discordantly overlie the metasedimentary rocks of the SGC and form discontinuous elongated folds oriented NW-SE, which form steep valleys.

The western and southern Meso-Cenozoic Borders were formed after Palaeozoic times and are mainly composed by sandstones and limestones that mark sea level oscillations during the Mesozoic and the following Cenozoic transgressions over the Hercynian continent. The existence of salt diapers in the western Meso-Cenozoic Border has a strong influence upon several hot springs, which show higher water flows and mineralisations than in the Hesperic Massif. Both borders are controlled by several fault systems and, in general, they are good prospects for the exploitation of deep-seated aquifers of non-convective type linked to permeable horizons.

The Lower Tagus and Sado Rivers Tertiary basins are composed by Miocene and Pliocene sediments (sandstones and porous limestones), which reach depths not deeper than 1400 m.

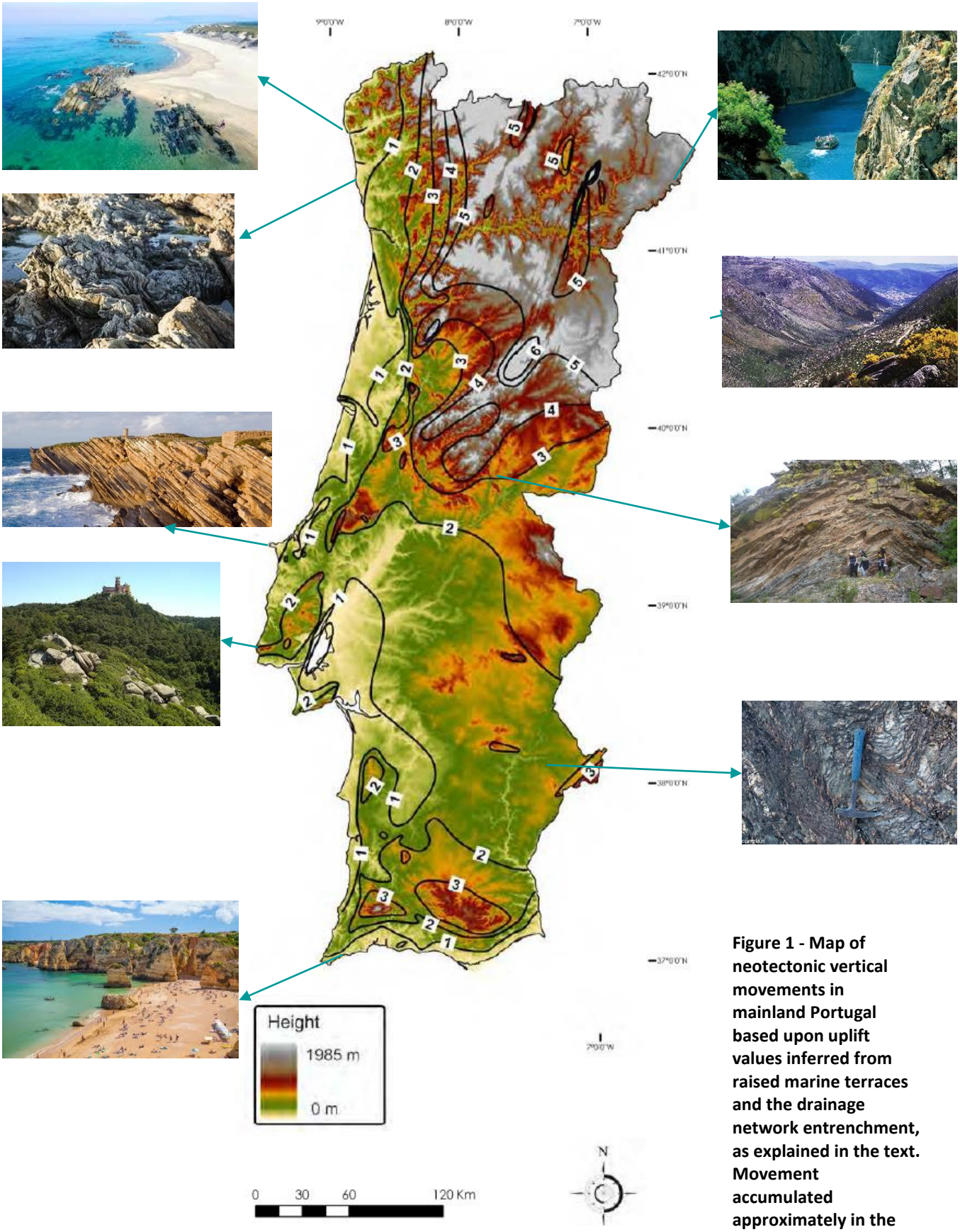

Figure 1 - Map of neotectonic vertical movements in mainland Portugal based upon uplift values inferred from raised marine terraces and the drainage network entrenchment, as explained in the text. Movement accumulated approximately in the last 3 Ma; uplift isolines in hundreds of meters (Cabral, 2012).

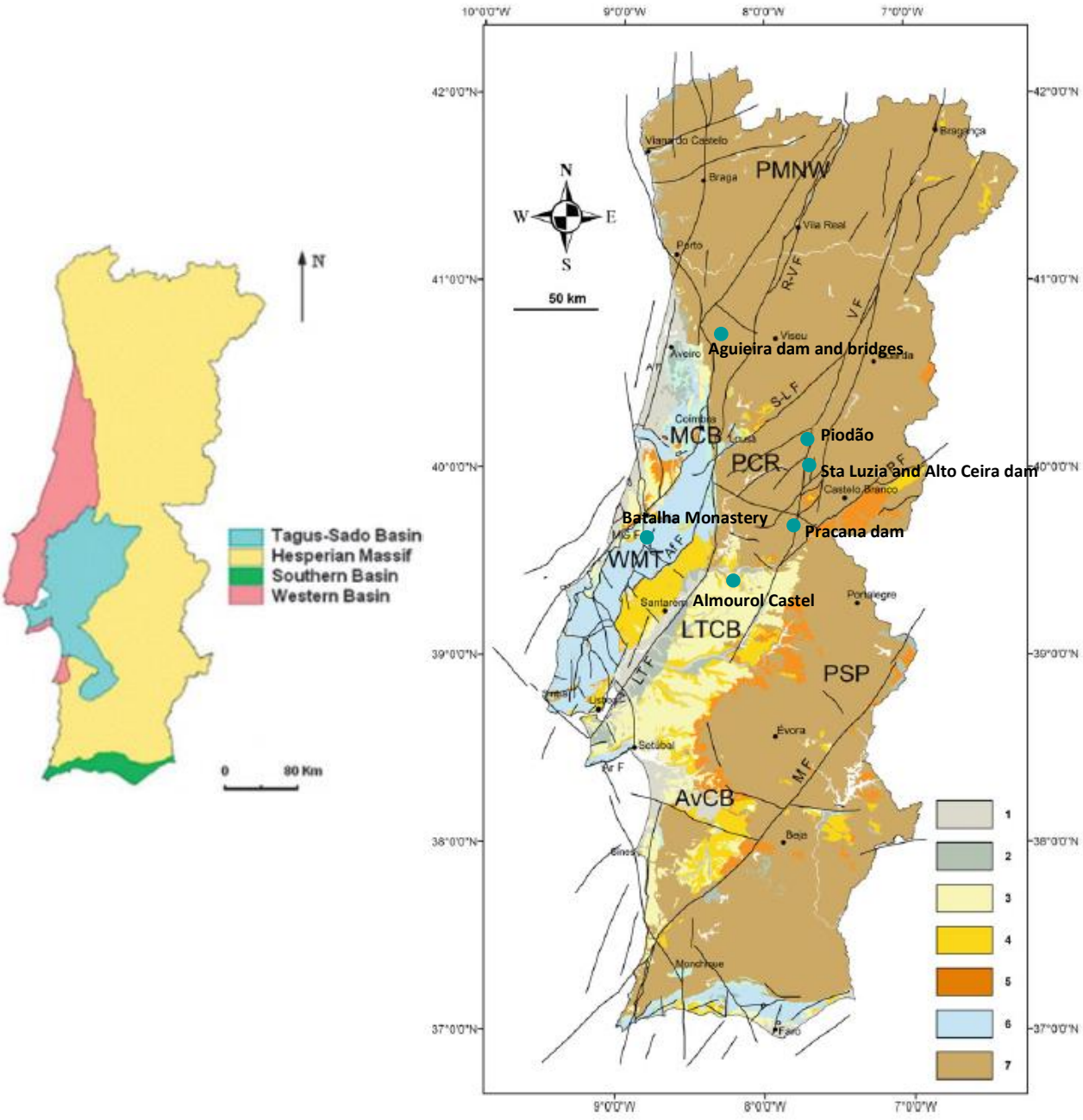

Figure 2 - General map of Cenozoic basins and main geological units of mainland Portugal. Legend: 1— Holocene; 2— Pleistocene; 3—Pliocene; 4— Miocene; 5—Paleogene; 6— Mesozoic; 7—Paleozoic and Proterozoic. Abbreviations: PMNW Plateaus and Mountains of NW Portugal; MCB Mondego Cenozoic Basin; PCR Portuguese Central Range; WMT Western Mesozoic Terrains; LTCB Lower Tejo Cenozoic Basin; AvCB Alvalade Cenozoic Basin; PSP Plateaus of Southern Portugal; A F Aveiro Fault; Af F Arrife Fault; Ar F Arrábida Fault; LT F Lower Tejo Fault Zone; M F Messejana Fault; MG F Marinha Grande Fault; P F Ponsul Fault; R-V F Penacova– Régua–Vérin Fault; S-L F Seia– Lousã Fault; V F Bragança– Vilariça–Manteigas Fault (Cunha, 2019).

2. Detailed program

June 3

8:00	Departure from LNEC
10:00	Monastery of Batalha
13:30	Lunch at the restaurant Cota Máxima (Aguieira Reservoir area)
15:30	ASR damaged bridges (Aguieira Reservoir area)
20:00	Dinner at the restaurant Quinta do Medronheiro Resort (Viseu)
23:00	Accommodation at Grão Vasco Hotel (Viseu)

June 4

8:30	Departure from the hotel
10:00	Piodão historical village
12:00	Alto Ceira dam
14:00	Lunch at the restaurant O Pascoal (Pampilhosa da Serra)
16:00	Santa Luzia dam
18:30	Departure to Castelo Branco
20:00	Dinner at the restaurant O Lagar (Herdade do Regato)
22:30	Accommodation at Hotel Melia (Castelo Branco)

June 5

9:00	Departure from the hotel
10:00	Pracana dam
14:30	Lunch at the restaurant Trincadela (Abrantes)
17:00	Almourol Castle
19:00	Arrival in Lisbon

3.1 Monastery of Batalha *(https://whc.unesco.org/en/list/264/)*

The Monastery of the Dominicans of Batalha was built to commemorate the victory of the Portuguese over the Castilians at the battle of Aljubarrota in 1385. It was to be the Portuguese monarchy's main building project for the next two centuries. Here a highly original, national Gothic style evolved, profoundly influenced by Manueline art, as demonstrated by its masterpiece, the Royal Cloister.

The design has been attributed to the English architect Master Huguet. The chapel's floor plan consists of an octagonal space inserted in a square, creating two separate volumes that combine most harmoniously. The ceiling consists of an eight-point star-shaped lantern. The most dramatic feature is to be found in the centre of the chapel: the enormous medieval tomb of Dom João I and his wife, Queen Philippa of Lancaster. Bays in the chapel walls contain the tombs of their sons, among them Prince Henry the Navigator.

The monastery of Batalha was the Portuguese center for the creation of stained glass, in the 15th and 16th centuries, where most of the practitioners of that art settled, who moved from here to other parts of the country.

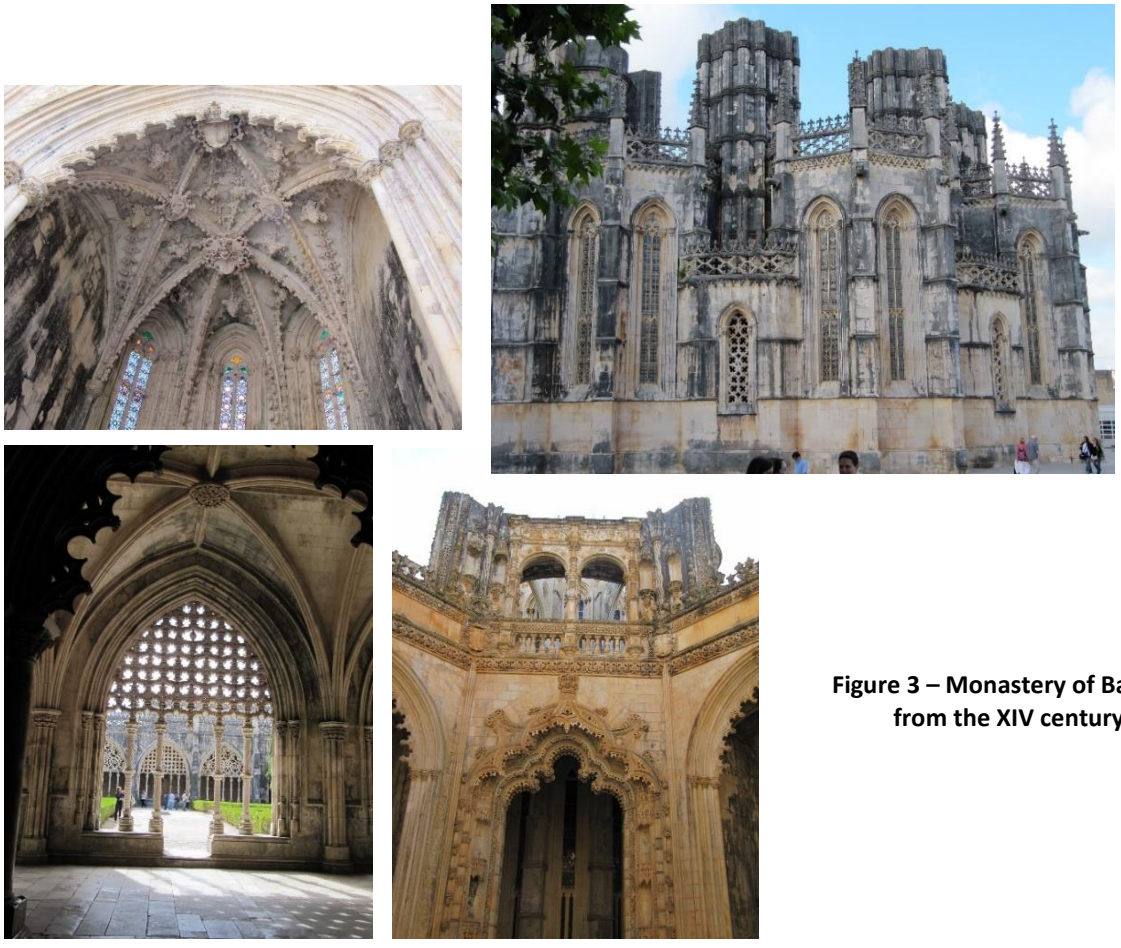

Figure 3 – Monastery of Batalha, from the XIV century.

3.2 Lunch at Cota Máxima restaurant *(https://www.cotamaxima.com/)*

Figure 4 – Cota Máxima restaurant is located at the margin of Dão river, in the reservoir of Aguieira dam.

3.3 Aguieira bridges

The Aguieira dam (Fig. 5), located in the centre of Portugal, was built from 1976 to 1979. The road network in its reservoir includes seven bridges, which share the same structural solution. Table 1 presents the number of spans, the total length and the height of the tallest pier of each bridge.

Figure 5 - Aguieira dam and image of part of the reservoir showing one of the seven bridges.

A detailed assessment of the concrete was performed by LNEC, in several studies carried out between 2009 and 2016, as reported by (Rodrigues et al., 2022):

- Mineralogical analysis by X-ray diffractometry;
- Petrographic characterization;

- Determination of soluble alkalis content;
- Determination of cement content;
- Determination of sulfate content;
- Potential residual expansion due to ASR;
- Potential residual expansion due to DEF;
- Microstructural analysis by SEM (electronic scanning microscopy);
- Evaluation of compressive strength;
- Evaluation of the elasticity modulus;
- Determination of stiffness degradation.

Table 1 – Aguieira bridges. Number of spans, total length and highest pier of each bridge (Rodrigues et al., 2021).

Bridge	Cunhedo	Mortágua	Foz do Dão	Santa Comba Dão	Criz I	Criz II	São João de Areias
Number of spans	9	5	9	5	5	8	7
Total length [m]	340	180	340	180	180	300	260
Highest Pier [m]	25	29	85	31	39	69	51

The laboratory tests, conducted on those studies, diagnosed both Alkali-Aggregate Reaction (AAR) and Internal Sulphate Reaction (ISR) due to Delayed Ettringite Formation (DEF) as the causes of deterioration, as mentioned in (Santos et al., 2022). The results of the tests performed by LNEC showed that the deterioration mechanism led to a significant change in the concrete mechanical properties, particularly the elasticity modulus, which conducted to the structural rehabilitation and reinforcement of 6 bridges and the replacement of Foz do Dão bridge, which was intensely deteriorated (Fig. 6).

The AAR was attributed to the use of alkali reactive aggregates, mainly quartzitic and granitic types. The aggregates have also been an internal source of alkalis, since the measured levels of soluble alkalis in extracted concrete samples, expressed as Na_2O_{eq}, ranges from 0.93 to 8.13 (3.44 in average) kg/m^3 of concrete, as noted in (Santos et al., 2022).

The ISR in these bridges was attributed to the high cement content employed, associated to the massive structural elements (foundations, piers and crossbeams). Although scarce information was available regarding the type of cement employed, the determinations of cement content in the samples extracted confirm high dosages in some parts (higher than 400 kg/m^3), as well as high cement SO_3 contents (values between 1.48% and 4.44%).

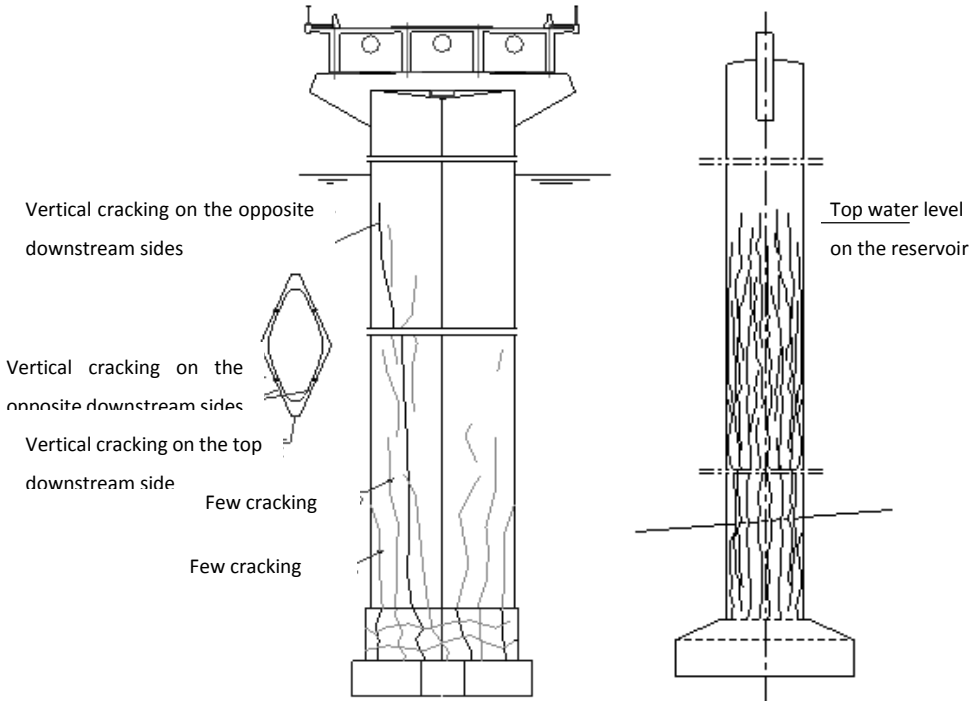

Figure 6 - Cracking observed on Foz Dão bridge piers (in Rodrigues et al., 2022).

The project for the rehabilitation of the six bridges comprised an inspection and a testing campaign. Deterioration manifestations were identified in the bridge piers (Rodrigues et al., 2022), namely:

- Several cracks in piers foundation, particularly at the basement level, with random orientation;
- Vertical cracking, mainly in the pier/basement connection, over all the piers perimeter, with uniform spacing;
- Vertical cracking in the piers shaft, with some spot zones with steel corrosion and deficient concrete joints.

The design of piers and foundations strengthening was based on the assumption that it was possible to maintain the decks, and that this approach was more competitive, in economic terms, than the integral replacement of the bridges. Only for the Foz do Dão bridge was verified to be more advantageous, in technical and economic terms, the integral bridge replacement solution.

In three of the bridges, it was decided to mechanically substitute the cylindrical piers by building a new annular cross section independent pier surrounding the old shaft. Micropiles were executed through the existing footings to support the new footings. These new piers were designed to have sufficient strength to support by themselves the deck, as it will be necessary in the case of the total loss of the original piers.

The rehabilitation of the three remaining bridges (Criz I, Criz II and São João das Areias) was based on a single structural solution: the construction of six piles with a metallic casing around each pier and

the corresponding pile cap. The pile cap has a prestressed connection with the pier in order to support the pier load when the stiffness of the immersed part of the pier decreases due to the swelling reactions. Additionally, a concrete covering was applied in the upper part of the piers, above the pile cap.

In order to monitor the structural effects of these reactions, in two of these bridges, São João das Areias bridge and Criz II bridge, a structural health monitoring system was installed. The superstructure of both bridges is a 15.20 m wide continuous pre-stressed reinforced concrete slab supported by 4 beams with variable height (2.0 m to 2.50 m) and width (0.50 m to 0.30 m). The slab has also a variable thickness from 0.16 m to 0.25 m at the connection to the beams. Both decks have crossbeams in the support sections as well as at the third-span sections. The reinforced concrete piers are composed of a single shaft, with a hollow cross-section, in the shape of a rhombus with sharp bevelled edges, inscribed in a 6.0 m × 3.0 m rectangle, with a wall thickness of 0.20 m. The bearings are placed on column heads, whose height varies between 1.00 m and 3.00 m and with a thickness of 0.80 m.

The Technical Visit program includes a visit to Foz do Dão bridge and Criz II bridge.

Foz do Dão bridge

The Foz do Dão bridge was replaced due to the intense deterioration, as mentioned before. Figure 7 shows a general view of both bridges: the old bridge (to be demolished) in the foreground and the new bridge in the background.

Figure 7 – Foz do Dão bridges: the old bridge in the foreground and the new bridge behind.

Criz I and Criz II bridges

The first rehabilitation works on Criz II bridge were carried out between 2007 and 2010, involving the abutments and the deck, including the application of external prestressing in the deck, due to the poor performance of the original prestress system, as well the replacement of the bearing devices and the

installation of damping devices in one abutment to improve seismic performance (pier P3). Fig. 8 and 9 illustrate different aspects of the Criz II bridge.

Figure 8 - Criz II bridge before and at during the rehabilitation works (Santos et al., 2022).

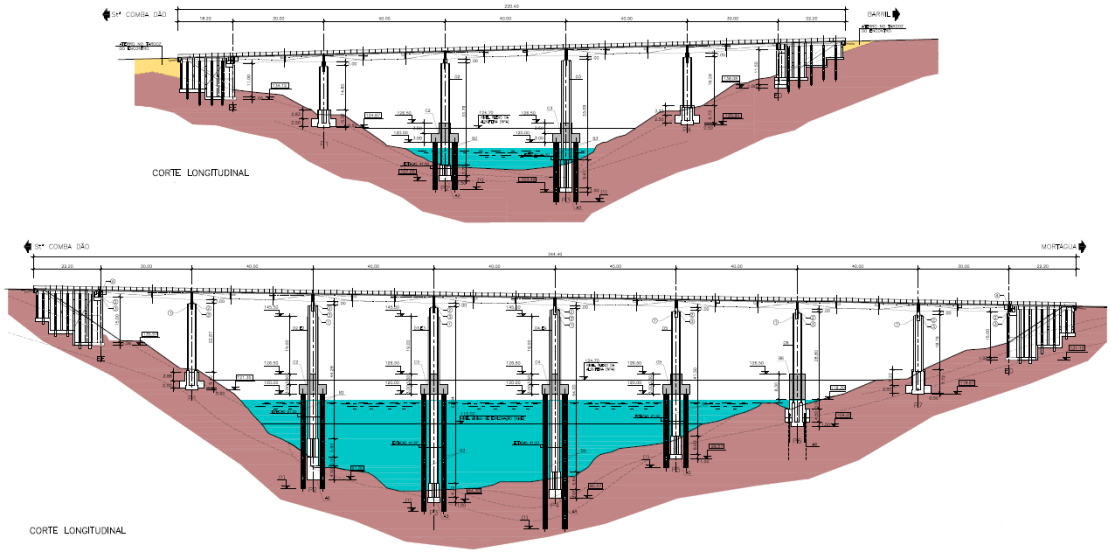

Figure 9 - Intervention solution in the foundations of Criz I and Criz II bridges (Rodrigues et al., 2022).

The structural solution designed for these bridges consisted of the deactivation of existing foundations and shaft pier sections that are immersed in the reservoir, through the execution of a set of several piles with ϕ1,50 m, headed by a prestressed pile cap in reinforced concrete, transferring the load from the shafts to the new foundation.

Additionally, in P2, P3 and P4 piers of the Criz II bridge, the strengthening of the shaft through jacketing with reinforced concrete was designed, above the top of the pile cap. This reinforcement was

necessary due to the high stresses in the existing shaft, resulting from local vibration modes associated with the high mass of the pier and water, which exceed their resistant capacity.

The reinforcement of pier basements located outside the reservoir was designed through external and internal jacketing with reinforced concrete, in order to protect these elements against water, and through prestress to confine and to able the load transfer between the pier and the new concrete element. The structural health monitoring systems comprise the measurement of strains within the concrete of the piles of piers P2 and P3 of both bridges and the measurement of strains on the concrete surface in the lower part of the piers, below the pile caps.

The main difficulty of these solutions was related to the execution of the piles and their caps with the use of aquatic and underwater resources, in order to ensure the perfect embedding on the bed rock. To minimize the identified difficulties, during the construction phase a system to guide and fix pile tubes was performed near the bottom, around the shaft and pier basement which also served as pier base confinement.

After finishing the new foundations and the piers jacketing, works were foreseen to repair and reinforce the piers shafts and beam caps, including coating and the application of water-leaking impregnation.

Finally, the replacement of bearings was decided, which included the construction of a new concrete element on the pier cap beams to support the deck during this work.

3.4 Dinner at Quinta do Medronheiro *(https://www.quintadomedronheiro.pt/)*

At Quinta do Medronheiro, where the vineyards meet between pine and forest. Touriga Nacional, Tinta Roriz, Jaen and Encruzado grown in granitic soil, give rise to wines of high character and longevity. The wines produced here honestly and sincerely express the place where the vines flourish, always elegant, deep, rich and with great personality.

They convey charm and pleasure to those who taste them.

Figure 10 – Images of Quinta do Medronheiro.

4.1 Piodão village *(https://www.centerofportugal.com/poi/piodao)*

Beautifully built upon the ledges which climb Serra do Açor, the village of Piódão is harmoniously craved into the nature that surrounds it and of which it seems to be a part. Its schist houses with slate roofs, which blend with the irregular pavement of the streets and with the colours of the mountain, are connected by stairs which overcome the unevenness of the ground.

In the early middle ages, the urban centre was at Casal de Piodão, in a valley located near the current village, but this settlement had to be moved because a Cistercian abbey, of which nothing remains, was built on that spot. Taken away from their land, the inhabitants settled in the southern slope of the mountain, probably around the 15th century. It was there that, over time, ledge by ledge, they built this incredibly beautiful mountain village.

The isolation to which difficult access routes have condemned Piodão throughout many centuries, has resulted in the medieval feeling of its streets, so you should take a walk through its steep streets, climb stairs and slopes while visiting the schist houses which are sometimes interrupted by a white church. When you go back, you should take a typical souvenir of this village: chestnut liqueur, honey spirits or a schist miniature of one of Piodão's typical houses (Fig. 11).

Figure 11 – Images of Piodão schist village.

4.2 Alto Ceira dam

The Alto Ceira dam was built between 1940 and 1949, with the first impounding of the reservoir occurring on March 1950 (Custódio et al., 2020). The thickness of the central cantilever varied between 4.5 m in the base and 1.5 m at the crest, and the dam crest had a development of 120 m, with maximum height of 37 m.

The first evidences of structural anomalies of Alto Ceira dam were observed during the first filling of the reservoir, and have increased since then. The anomalous dam behaviour was characterized by progressive horizontal upstream displacements, progressive upward vertical displacements and intensive cracking. Many studies and tests have been carried out in order to get a better knowledge of the causes of the structural problems. Alkali-aggregate reactions (AAR) in the concrete have been identified as the main cause of the intensive cracking of the thin arch dam structure (Figure 12) (Ramos et al., 1995; Custódio et al., 2020).

Figure 12 - Alto Ceira dam. General view and detail with extensive cracking and exudation (COST TU1402: Quantifying the Value of Structural Health Monitoring).

Samples of concrete were collected in 1951 and in 1986 (Fig. 13) to determine the elasticity modulus and the compressive strength of the concrete and it was concluded that at the time the sampling was performed, the concrete was already altered; especially in locations L1 (-29 %), L2 (-26 %) and L5 (-33%). In terms of alteration, the concrete from locations L1 and L5 (block BC, close to joint C) seems to be the most affected, followed closely by that from location L2 (block DE, close to joint D); the concrete from location L3 (block FG, close to joint F) appeared to be the much less altered or not altered at all (+13 %). The results of the mechanical tests show variation for the different areas

sampled (Table 2). The results also suggest that different concrete strength classes might have been used in the sampled locations.

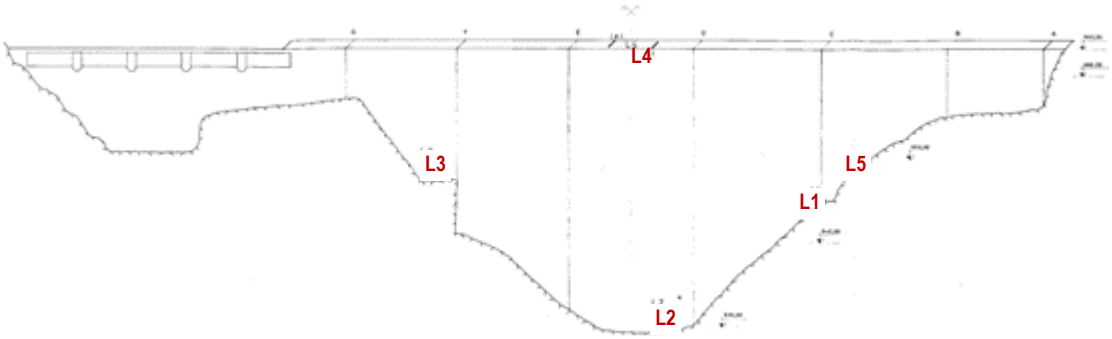

Fig. 13 – Alto Ceira dam. Identification of the core extraction locations, in 1986 (Custódio et al., 2020).

Table 2 – Alto Ceira dam. Modulus of elasticity and compressive strength of the dam's concrete, assessed in samples collected in 1986 (Custódio et al., 2020).

Location	Specimen	Diameter, Ø (mm)	Height, h (mm)	Modulus of elasticity (GPa)			Compressive strength (MPa)		
L1	1	150	400	23.6	24.8		39.3	43.6	
	2	150	400	26.1			47.9		
L2	3	150	400	28.1	26.3		44.9	45.6	
	4	150	400	24.4		27.3	46.4		39.4
L3	5	150	400	33.1	35.8		33.1	31.9	
	6	150	400	38.5			30.6		
L5	7	150	400	25.7	22.2		38.2	36.5	
	8	150	400	18.7			34.7		

The macroscopic observation and the petrographic examination revealed that coarse and fine aggregate have a similar mineralogical composition, *i.e.* siliceous (quartzite and quartz) and silicate (metapelite, feldspar, mica) *latu senso*. It was noticed that the coarse aggregate was obtained by crushing of quarzitic blocks, the fine aggregate was composed of alluvial sand (river sand) and particles resulting from crushing quarzitic rock to produce the coarse aggregate (Custódio et al., 2020).

The tests performed have shown that the aggregates in the concrete sampled from the dam still exhibited potential for residual expansion due to ASR, and that this potential was higher on the dam's right bank. Considering that all the concrete had, initially, a similar ASR potential, the results suggest that the concrete from zone I, above the maximum retention level, expanded the least during the 40 years' period, the concrete from zone II, between the minimum and maximum exploration level, expanded the most in that period, and that the concrete sampled from zone III, permanently submerged, presented an intermediate expansion level. Hence, the concrete from the left bank might have expanded more during the referred period.

In 2012, Batista and Piteira Gomes reported the main internal swelling mechanism involved and the predicted vertical strains associated to the concrete swelling. The results, summarized in Table 3, show an average vertical strain rate in the previous 5 years before 2012, of 10 to 120x10^{-6}/year and an accumulated vertical displacement ranging from 600 to 4600x10^{-6}, until 2012 (Batista and Piteira-Gomes, 2012).

Table 3 – Alto Ceira dam. Reaction type and vertical strains due to swelling (Batista and Piteira-Gomes, 2012).

Main aggregate type		Swelling phenomenon	Accumulated vertical strain until 2012 (x10^{-6})	Average annual rate in the last 5 years, before 2012 (x10^{-6})
Coarse	Fine			
Quartzite	Quartzite	Alkali-silica reaction	4600 – 600	120 – 10

The cracking condition of the dam body, assessed in 1986, 1994 and 2001, allowed to verify that:

- Between 1986 and 1994 there was no increase in the number of structural cracks, however an increase in the opening of the existing cracks was observed in that period, mainly at the upper levels of the FG block, above the 660 m elevation;
- Between 1994 and 2001, there was an important increase in the number of structural cracks. In some cases, they resulted from the prolongation of the existing cracks observed in 1994;
- There were several cracks in the upstream face, especially near the right abutment;
- Some cracks had significant openings (mainly between 1 and 3 mm) and depths (mainly up to 60 cm). Several cracks were wet, revealing leakage problems throughout the structure.

In addition to these specific reports, visual inspections during dam's life allowed to monitor the progress of the intensive cracking in the dam body (Fig. 14 and 15).

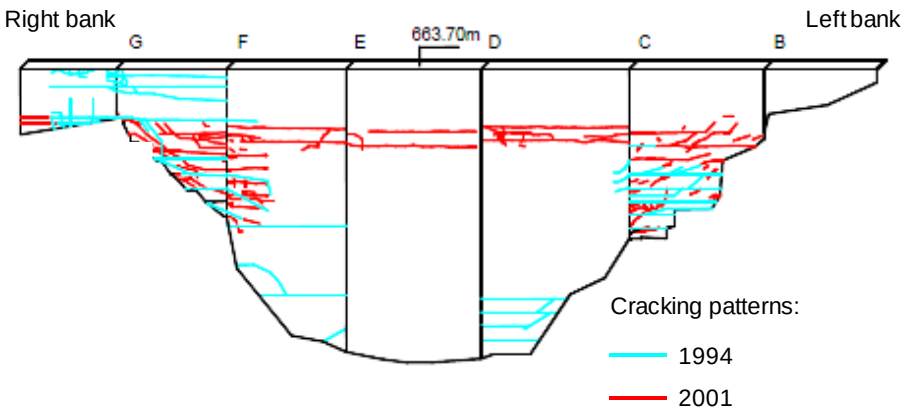

Fig. 14 – Alto Ceira dam. Evolution of the cracking condition between 1994 and 2001 (Custódio et al., 2020).

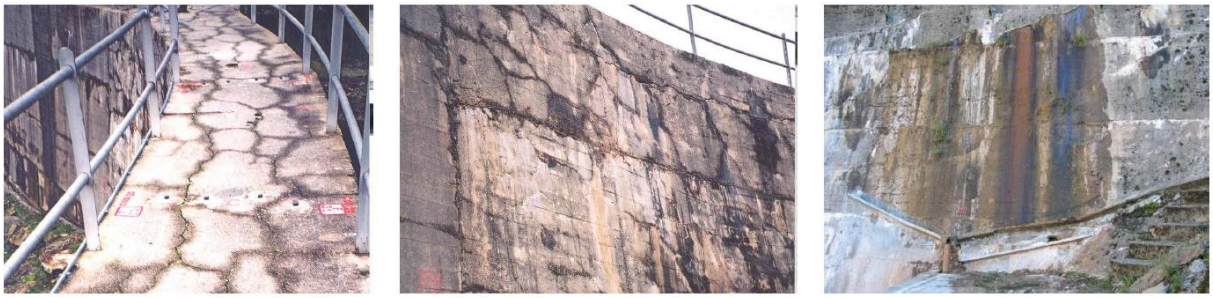

Fig. 15 – Alto Ceira dam. Cracking patterns on the crest and on the downstream surface, and device to measure the leakage through the dam's body (Custódio et al., 2020).

The various tests conducted in-situ and in the laboratory, to concrete samples extracted from the dam, allowed determining that (Custódio et al., 2020):

(i) The aggregate has potentially alkali-reactive constituents and also constituents that may release alkalis into the concrete pore solution, which in turn will promote ASR development;

(ii) Although the petrographic analysis indicated the aggregate was potentially alkali-reactive, the aggregate used in the dam has passed the chemical test method for potential alkali-silica reactivity of aggregates, done in 1990, illustrating the lack of reliability of that method, which was eventually withdrawn by ASTM in 2016;

(iii) The swelling observed in the dam was due to the deleterious development of ASR in the concrete;

(iv) The residual expansion tests, carried out in 1990, showed that the concrete still had residual expansion potential; behaviour which was corroborated later on by the intensification of cracking in the structure, ultrasonic testing and the structural monitoring;

(v) ASR development has resulted in a relevant increase in the travel time of the ultrasonic wave pulse between the transducers, which evolved throughout the dam's service life;

(vi) ASR has evolved to an extent so that it resulted in a detectable reduction of the concrete compressive strength, in some of the assessed locations;

(vii) The SDT evidenced that ASR has resulted in a relevant decrease in the modulus of elasticity of the concrete in all locations sampled;

(viii) In terms of the concrete alteration, it was found that, from all sampled locations, the most altered concrete was that from locations L3 and L5 (in block FG);

(ix) The SDT allowed to estimate that, in average, ASR is likely to have caused, in the sampled concrete, an expansion that, in unrestrained conditions, would reach 1900×10^{-6};

(x) The ASR induced expansion and cracking of the concrete, which has led to a reduction in the service life of the structure.

Qualitatively, there was a correlation between the areas of the dam where large horizontal and vertical displacements were occurring and where cracking was most severe, especially in the upstream

face and where the lowest mechanical properties and the highest total non-restrained expansion values were obtained. An overall analysis of the dam's condition suggests that higher expansions in that area could be due to the higher solar incidence (since the right abutment is facing south), to the easier access to water (since the cracking in the upstream face was also more pronounced in the right abutment) or to the lower stresses in this abutment (result of the asymmetry of the valley).

As a result of reliability concerns, the possible need to abandon the dam and to build a new one 200 m downstream of the existing dam was reported to be under consideration. The old dam (Alto-Ceira) would serve as a cofferdam for the new dam (Fig. 16).

The new Alto Ceira dam was concluded in 2024. It is a concrete arch dam with gravity abutments, 133 m crest length and a 41 m maximum height above the foundation level (Fig. 17).

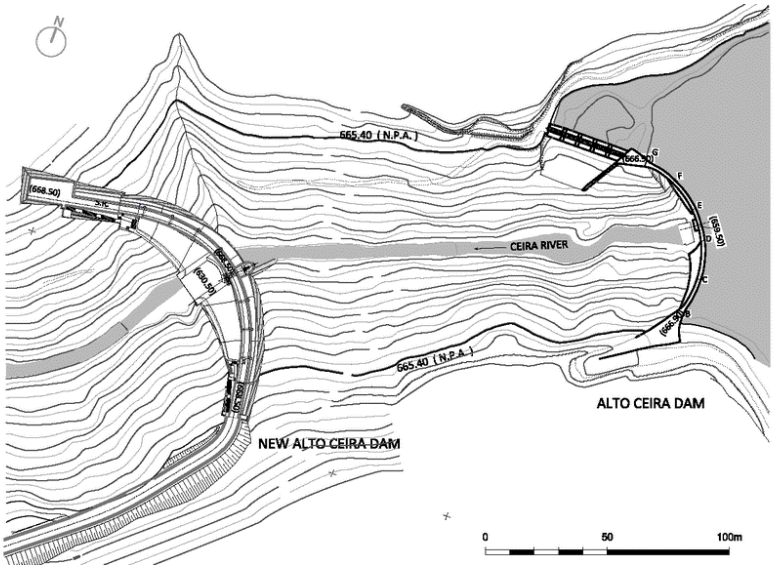

Figure 16 – The new Alto Ceira dam (left) and the upstream existing one (right) (Matos et al., 2012).

Figure 17 – The new Alto Ceira dam (Leitão et al., 2015).

4.3 Santa Luzia dam

The Santa Luzia dam was built between 1939 and April 1943 and consists of two concrete arch structures. The main structure, located in a narrow gorge, is a thin arch with 76 m maximum height and a variable thickness in elevation, with a minimum of 2.5 m at the crest and 13.0 m at the bottom, while the secondary structure consists of a 27 m high arch-gravity to close a left bank cavity at high elevation (Fig. 18). A V shaped buttress extends the main structure, functioning as an abutment. The rock mass foundation is heterogeneous and mainly consists of quartzites, except at the bottom of the valley and at the upper zone of the left bank, where quartzitic conglomerates occur. The first filling of the reservoir began in October 1942 and since then the dam has been continuously in operation, with several significant drawdown of the water level in the reservoir, particularly in the period between 1942 and 1959.

Figure 18 – Santa Luzia dam. General view and cross section of the central cantilever (Batista, 2022).

The available data about the composition and properties of the concrete are very reduced. The Portland cement mean contents was about 240 Kg/m^3 and quartzite aggregates were used in the dam's concrete mix.

The first signs of the swelling phenomena were identified in 1966, from the results of several geodetic surveys, due to the existence of progressive displacements at the crest, vertical upwards and radial upstream. Linear cracking at the downstream surface, parallel to the foundation, was also detected some years later (Fig. 19).

In 1995, three vertical cores, from the crest of the main arch, with 47 m depth, and a core in the arch-gravity, with 17 m depth, were drilled. This study allowed the identification of products resulting from

alkali-silica reactions, as well as the presence of ettringite and thaumasite, resulting from internal sulphate reactions.

The analysis done to the cement paste led to conclude that a low alkali content cement was used in the concrete mix. The swelling tests, performed at 38ºC constant temperature, on specimens soaked in sodium hydroxide and potassium hydroxide solutions, showed, for a concrete about 50 years old, low residual swelling, of about 100×10^{-6}. Physical tests were also performed to characterize the concrete structural properties

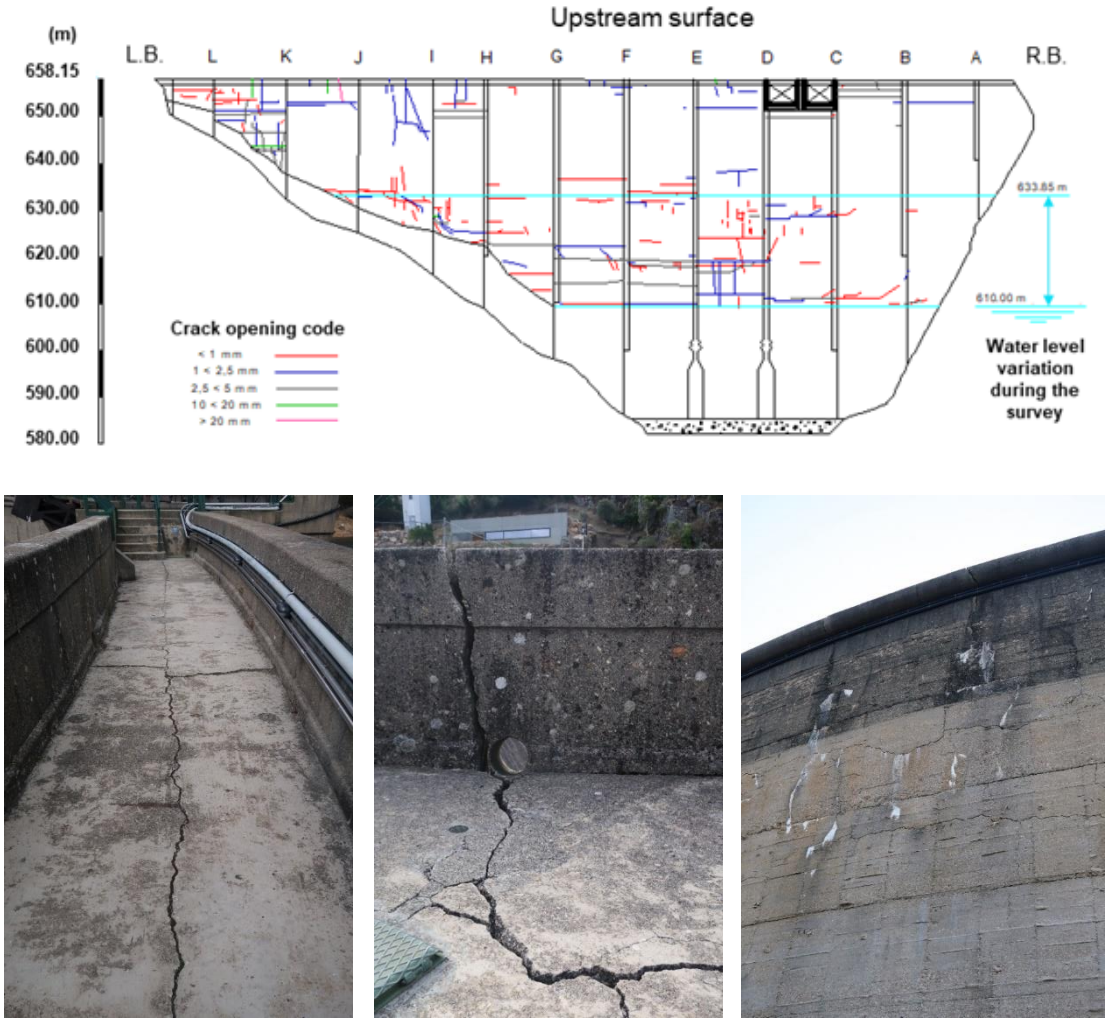

Figure 19 – Santa Luzia dam. Results of crack survey of upstream surface due in October 1998 (Piteira-Gomes et al., 2022a; Batista, 2022).

The monitoring system has undergone several improvements over the years, because this was the first large concrete arch dam built in Portugal, where the first steps in dam's monitoring took place and it was necessary to introduce technological innovations that meanwhile appeared.

Figure 20 shows the current monitoring system for measuring horizontal displacements (plumb lines and geodesy) and vertical displacements at the crest (levelling line and R13 rod extensometer).

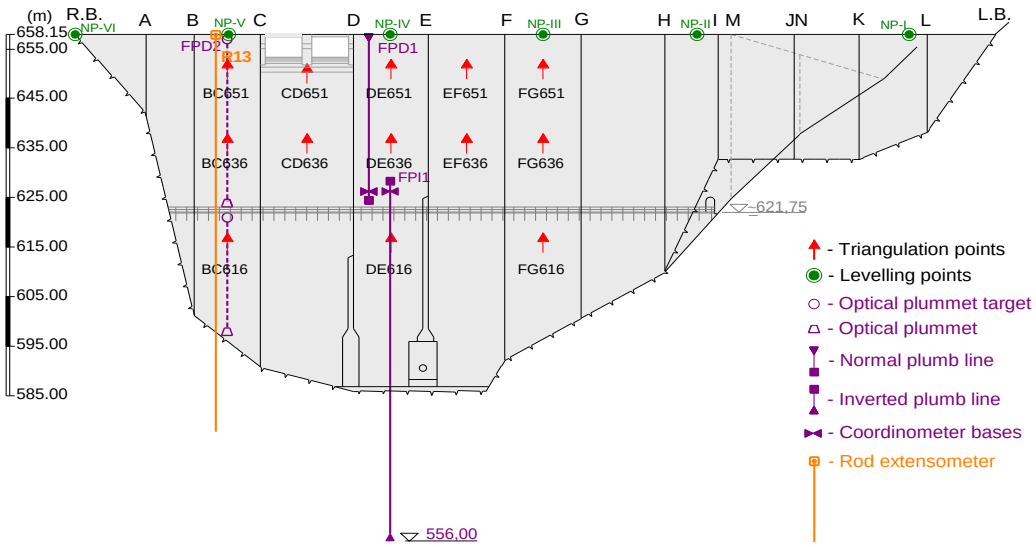

Figure 20 – Santa Luzia dam. Monitoring instruments to measure horizontal displacements in the main arch and vertical displacements at the dam's crest (Piteira-Gomes et al., 2022a).

The displacements monitoring system of Santa Luzia dam was ruled, over a long period, from 1943 to 1997, only by geodetic methods, namely by horizontal displacements by triangulation on the main arch, since February 1943, and vertical displacements at crest by precision levelling, since October 1945. The foundation displacements measurements, by rod-extensometers, started in November 1987. In November 1988, the existing levelling line at crest was reformulated, with the introduction of new marks on the intermediate blocks. Finally, the monitoring of horizontal displacements by a plumb line placed in the block DE began in August 1997. The frequency of geodetic observation campaigns was not very regular, mainly in the first period between 1943 and 1970, in which 14 campaigns were carried out in 27 years but in the period between 1948 and 1959 there were no monitoring. It was from 1983 that geodetic campaigns began to be carried out with greater regularity, on an annual basis, although with some few years in which geodetic surveys were not performed.

In Figure 21 the irreversible vertical displacements at the six marks at crest are presented, due to swelling process, at the end of the second and third analysis periods. Although the elapsed time in the third period is less, it can be concluded that there was a significant attenuation of the swelling process, while not homogeneous.

The analysis carried out through the application of statistical methods to the displacements observed in three distinct and relatively long periods, with similar duration, allowed to get information about time periods with different structural behavior and also to have a global pattern of how the concrete deterioration process developed, due to internal swelling reactions.

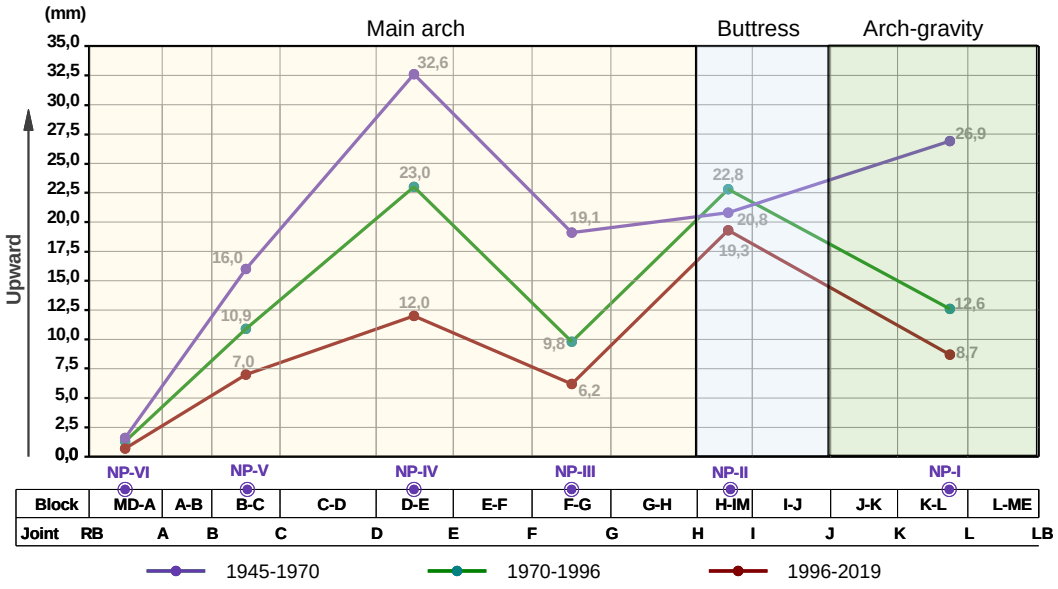

Figure 21 – Santa Luzia dam. Irreversible vertical displacements computed for the levelling marks at the crest in the three periods of analysis (Piteira-Gomes et al., 2021a).

The analysis of the horizontal displacements only assesses the behavior of the main arch, showing that in the first period, from 1943 to 1970, there was greater stiffness of this structural part to the hydrostatic pressure action. It was in the second period, from 1970 to 1996, that loss of stiffness occurred due to cracking occurred. Regarding the irreversible displacements in the upstream direction, it was clear that its progression rate was higher in the second period, compatible with the loss of the structural stiffness, and also that in the third period there was a very significant attenuation of these displacements, configuring a possible exhaustion of the swelling reaction.

The analysis of the vertical displacements allows the assessment of the behavior of the three structural elements, the main arch, the arch-gravity and the buttress, which shows that there was a reduction in the irreversible vertical crest displacements upwards from the first to the second period and from the second to the third period, with exception of the buttress, where the values have been very similar. It also shows that in the first period, between 1943 and 1970, the time effects attributable to the swelling process had some expression in the main arch and in the buttress, with average annual rates between $9x10^{-6}$ and $18x10^{-6}$, but a much more expressive development was recorded in the arch-gravity structure, with irreversible vertical strains greater than $1200x10^{-6}$, at the block KL, and with an average annual rate four times higher than the average value developed in the other structural elements. These results corroborate with the appearance of horizontal cracks reported in several documents, the first one related with the visual inspection carried out during the drawdowns of the water level in September 1959. Finally, it is important to mention that the analysis of vertical displacements also reveals a significant reduction in progression rates in the third period, which is compatible with the swelling reactions exhaustion.

4.4 Dinner at restaurant O Lagar - Herdade do Regato

(http://herdadedoregato.com/a-herdade/galeria/a-herdade/)

Enriched by history, the old olive oil mill was converted into a Restaurant-Museum, full of symbolism and human ingenuity.

Figure 22 – Images of Herdade do Regato.

5.1 Pracana dam

The Pracana dam is a buttress structure, 60 m high, completed in 1951. The dam is founded on a rock mass of phyllite and greywacke alternations and was built with a concrete mix including quartzite and granite aggregates. An abnormal behaviour of the dam was observed since the first filling of its reservoir in 1951, characterized by progressive vertical and axial horizontal displacements (upstream-downstream direction) and extensive cracking. Physical and chemical tests performed over time, on samples taken from the dam´s body, confirmed the existence of ISR-ASR of great magnitude. At the end of the eighties of the last century the reservoir remained empty, to allow large scale rehabilitation works that have been implemented from 1988 to 1992 (Fig. 23).

Figure 23 – Pracana dam. Map cracking of the downstream and upstream faces.

In Table 4, the results of quantitative interpretation of vertical displacements, obtained from the crest levelling before and after the dam rehabilitation, are compared. These two periods have similar duration and the results clearly show that the accumulated swelling and the expansion average annual rates are significantly lower in the second period, with exception of block B1. In all buttresses with

monitored results in both periods there were reductions between 5 and 8 times and in block B14, on the left bank, there was a reduction of 2.5 times. However, in block B1, on the right bank, there was an increase of about 40% in the annual swelling rate.

Block B15, on the left bank, is the one with the greatest irreversible deformations (it was not monitored in the first period of the dam's life).

Table 4 – Pracana dam. Average swelling accumulated and average annual rates, during the periods of 1952-1980 and 1992-2019, obtained through the analysis of the crest vertical displacements (levelling) (Batista, 2022).

Buttress	Height (m)	First period (October 1952 to May 1980)			Second period (December 1992 to January 2019)		
		Accumulated vertical displacements (mm)	Accumulated vertical strain ($x10^{-6}$)	Annual swelling rate ($x10^{-6}$)	Accumulated vertical displacements (mm)	Accumulated vertical strain ($x10^{-6}$)	Annual swelling rate ($x10^{-6}$)
B2	3.7	-	-	-	2.7	716	27.4
B1	10.8	5.6	521	18.4	7.4	684	26.2
B0	17.2	-	-	-	6,0	349	13.4
P1	25.1	-	-	-	4.9	195	7.5
P2	32.1	33.1	1050	37.1	4.4	137	5.3
P3	38.6	-	-	-	3.0	76	2.9
P4	47.3	29.0	607	21.5	3.2	67	2.6
P5	57.8	-	-	-	4.2	73	2.8
P6	63,0	31.8	550	19.4	5.1	80	3.1
P7	62.3	-	-	-	5.5	88	3.4
P8	62.3	32.1	535	18.9	6.4	102	3.9
P9	62.3	-	-	-	5.5	88	3.4
P10	60.9	26.8	466	16.5	5.2	85	3.2
P11	53.4	33.1	685	24.2	6.3	117	4.5
P12	38.4	30.6	836	29.5	5.5	142	5.4
B13	24.2	-	-	-	3.3	134	5.1
B14	12.6	25.5	2024	71.5	9.3	734	28.1
B15	4.2	-	-	-	11.2	2667	102.2

The structural rehabilitation of the dam included the following works: i) general treatment of concrete, to its regeneration; ii) placement of an impermeable membrane on the upstream surface, including the construction of an upstream foundation plinth; ii) construction of two sets of concrete struts for locking the buttress webs at the foundation level, one next to the downstream toe and the other in an intermediate position; and iii) consolidation of the foundation and execution of new waterproofing and drainage curtains, being the last ones executed form the top of a plinth built along the dam upstream toe. The improvement of the monitoring system was also done.

The waterproofing system of the upstream surface consists of a Carpi patented system consisting of an impervious flexible PVC geomembrane 2.5 mm thick, heat-coupled during extrusion to a non-woven, needle-punched 500 g/m^2 geotextile (Fig. 24). The PVC geomembrane, which was applied over a HDPE geonet with drainage purpose, fulfil many requirements, namely: i) low permeability (k≈10^{-12} cm/s); ii) high flexibility, that enables installation also on not smooth faces; iii) resistance to punching, tearing and impact; iv) resistance to high temperature gradients and to freeze-thaw cycles; v)

resistance to stresses induced by large relative movements, such as movements induced by earthquakes; and vi) expected long durability.

Figure 24 – Pracana dam. Stage of installation of the upstream impervious membrane (Batista, 2022).

During the dam rehabilitation, the monitoring system was revised to conform with the Portuguese regulations for dam safety, which had been approved in the meantime, and also enhanced to better monitor the structural behaviour and the swelling process evolution (Figure 25). So, the following instruments have been introduced: i) multiple rod extensometers installed along the heads of five buttresses (P1, P4, P6, P9 and P12); ii) two rod extensometers on each buttress foundation, one near the head and other at the downstream toe; iii) inverted plumb lines in fife buttresses (P1, P4, P6, P9 and P12), with suspension near the dam crest and anchored into the foundation rock; iv) thermometers located inside two buttresses (P5 and P7); and v) new jointmeters to measure the relative movements of joints. The geodetic monitoring system was also revised and improved.

The monitoring system installed in Pracana dam indicates progressive upstream horizontal displacements and vertical upwards crest displacements. Interpretation of levelling, plumb lines and rod extensometers displacements by statistical models has shown that the swelling process, although still present, has a significant lower rate in relation to the first period of dam's operation, before the execution of the rehabilitation works.

In the first period of operation, the average vertical accumulated strain in the central seven monitored buttresses was 680×10^{-6}, corresponding to an annual swelling rate of 24×10^{-6}/year. In the second period of dam's operation the average vertical accumulated strain in the central twelve monitored buttresses was 105×10^{-6}, with an annual swelling rate of 4×10^{-6}/year. A swelling rate significant reduction of about six times was achieved with the rehabilitation works.

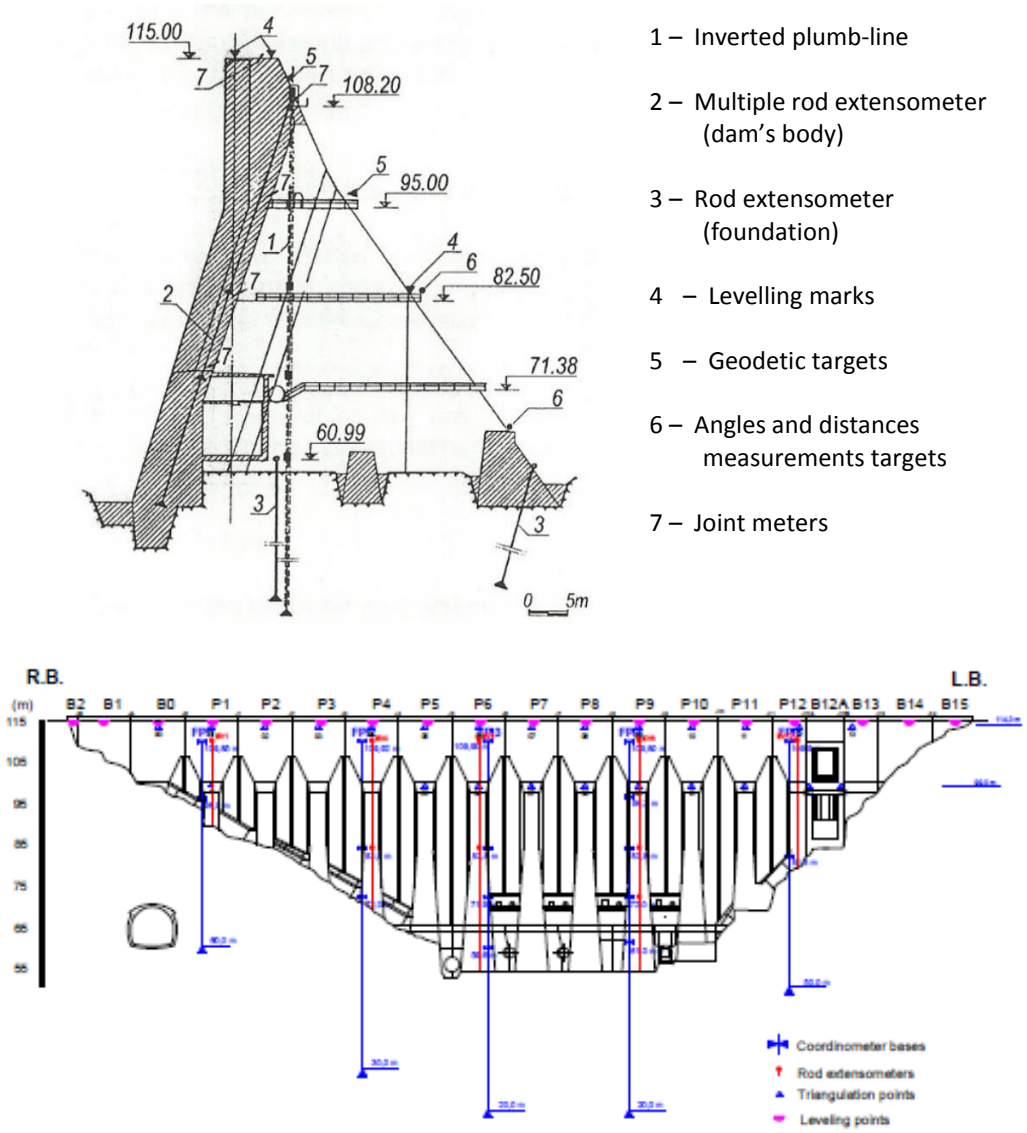

Figure 25 – Pracana dam. General scheme of the new monitoring instruments installed in 1992 to measure displacements of the dam and its foundation (Piteira-Gomes et al., 2022b).

The results for the side blocks B2, B1 and B0, located on the right bank, are similar in the two periods of dam's operation. In the first period the vertical accumulated strain of block B1 was 520×10^{-6}, with an annual swelling rate of 18×10^{-6}/year, and in the second period the corresponding values for the three blocks were 580×10^{-6} and 22×10^{-6}/year, respectively. However, this last value is five times higher than the correspondent value computed for the central zone.

Regarding the left bank, the comparison is made considering only the block B14 because it is the only one that was monitored in both periods and also because the results obtained in the three blocks B13, B14 and B15 are very different. Thus, in the first period vertical accumulated strain of block B14 was 2020×10^{-6}, with an annual swelling rate of 72×10^{-6}/year, and in the second period the average vertical accumulated strain in the same block was 730×10^{-6}, with an annual swelling rate of 28×10^{-6}/year.

However, vertical accumulated strain of block B15 during the second period was $2670x10^{-6}$, with an annual swelling rate of $100x10^{-6}$/year. This value is about 25 times higher than the expansions in the central zone, which require further investigation and, if necessary, a medium-term intervention.

Mitigation of the swelling process proportionate by the rehabilitation works is undoubtedly a positive result to which the geomembrane installation on the upstream surface has given an important contribution. However, the long period with the reservoir emptied and the dam weather conditions, relatively warm and dry, may have also contributed to reduce the speed of the swelling process. In view of the results obtained, it is considered that the geomembrane continues to exhibit a good performance and functionality, preventing the upstream water access to the dam body. After 28 years of natural exposure, the evaluation of its physical condition must be checked frequently, which is done by carrying out visual inspections, in order to detect rips usually caused by floating woody material, especially after the occurrence of important floods. These rips are usually repaired in the following dry season.

Finally, it must be recognized that the rehabilitation of the Pracana dam is a successful case, because since that time it has been operating without limitations. However, in addition to the implemented observation plan, which includes the analysis of the monitoring data and of the visual inspections, it is advisable to perform laboratorial tests for assessing the current situation of the swelling process and to predict its evolution, in order to ensure the safety of the dam.

5.2 Almourol Castel *(https://turismodocentro.pt/poi/castelo-de-almourol/)*

In the middle of the River Tagus, the enigmatic Almourol Castle is one of the most emblematic monuments of the Christian reconquest. Situated on an island in the middle of the River Tagus, Almourol is one of the most distinctive castles in Portugal, because of its historical significance and surrounding landscape.

Its history reminds us of the Reconquest of the Portuguese territory during the Middle Ages. When the Christians arrived here in 1129, the castle already existed under the name of Almorolan, having been incorporated immediately afterwards into the land that was placed under the protection of the Knights Templar, whose Master at that time was Gualdim Pais. According to an inscription at the entrance to the castle, its reconstruction work began in 1171.

After the Order of the Knights Templar was disbanded and the need to defend the territory no longer existed, the castle lay abandoned and forgotten until it was espoused by the prevailing Romantic spirit of the 19th century and restored to its present-day appearance.

Figure 26 – Almourol Castel in the Tagus river.

REFERENCES

Batista, A. L., 2022. Deterioration processes of dams affected by concrete swelling reactions. The Portuguese experience in monitoring and rehabilitation. Keynote Lecture, Proceedings of the 16th ICAAR, Lisbon.

Batista, A. L. & Piteira-Gomes, J., 2012. Practical assessment of the structural effects of swelling processes and updated inventory of the affected Portuguese concrete dams", in 54º Congresso Brasileiro do Concreto - CBC 2012. Maceió, Alagoas, Brasil.

Cabral J (2012) Neotectonics of mainland Portugal: state of the art and future perspectives. Journal of Iberian Geology 38 (1):71–84.

Correia, A., Ramalho, E.C., 2005. Updated Surface Heat Flow Density Map in Mainland Portugal. Proceedings World Geothermal Congress 2005, Antalya, Turkey.

Cunha, P.P. 2019. Cenozoic Basins of Western Iberia: Mondego, Lower Tejo and Alvalade basins. In: C. Quesada & J.T. Oliveira (eds). The Geology of Iberia: A Geodynamic Approach. Regional Geology Reviews, Springer International Publishing, Vol. 4 – Cenozoic Basins, Chapter 4, pp. 105-130.

Custódio, J., Mata, J., Serra, C., Bettencourt Ribeiro, A., & Tavares de Castro, A. 2020. The diagnosis and prognosis of ASR in dams. Application to Alto Ceira dam (Portugal). 4th International Dam World Conference - DW 2020, Lisbon, Portugal.

Leitão, N.S., Castro, A.T., Cunha, J.G, 2015. Analysis of the observed behaviour of Alto Ceira II Dam during the first filling of the reservoir. 2nd International Dam World conference, Lisbon.

Matos, D.S., Pimentel, R., Figueiras, J., Rodrigues, C., Faria, R., Castro, A.T. 2012. Novel fiber optic transducers embedded into concrete mass applied to the New Alto Ceira Dam. Dam World Conference. Maceió, Brazil.

Piteira-Gomes, J.P., Cunha, J.G., Batista, A.L., Almeida, F., 2022a. Monitoring and assessment of the structural effects due to ASR in Santa Luzia dam (Portugal). Proceedings of the 16th ICAAR, Lisbon.

Piteira-Gomes, J.P., Matos, D.S., Batista, A.L., Ferreira, I. 2022b. Structural behavior of Pracana dam 30 years after the large rehabilitation due to severe ISR-ASR damage. Proceedings of the 16th ICAAR, Lisbon.

Ramos, J.M., Batista, A.L., Oliveira, S.B., Castro, A.T., Silva, H.M., Pinho, J.S. 1995. Reliability of Arch Dams Subject to Concrete Swelling -Three Case Histories. Proceedings for the Second International

Conference on Alkali-Aggregate Reaction in Hydroelectric Plants and Dams, USCOLD, Chattanooga, Tennessee.

Rodrigues, T., Pereira, A.R., Costa, A. 20212. Reinforcement and replacement interventions in some bridges located on Aguieira Dam road network. Proceedings of the 16th ICAAR, Lisbon.

Santos, L.O., Xu, M., Santos Silva, A. 2022. Monitoring of ASR/ISR structural effects in Aguieira bridges. Proceedings of the 16th ICAAR, Lisbon.